









Cite this: *Chem. Soc. Rev.*, 2017, 46, 3886

## Expanding applications of SERS through versatile nanomaterials engineering

M. Fernanda Cardinal,  Emma Vander Ende, Ryan A. Hackler,   
 Michael O. McAnally,  Peter C. Stair,  George C. Schatz  and  
 Richard P. Van Duyne \*

Surface-enhanced Raman scattering (SERS) spectroscopy has evolved into a cross-disciplinary analytical technique by unveiling relevant chemical, biological, material, and structural information. The focus of this review is on two critical properties for successfully expanding applications of SERS spectroscopy: quality of the plasmonic substrate and molecule localization to the substrate. In this review, we discuss recent work on quantifying SERS distance dependence, key factors for substrate characterization and performance evaluation, expansion of SERS applications through substrate development for UV plasmonics and short-distance capture strategies for optimizing analyte-surface structures. After surveying the recent developments of these seemingly disparate fields, we suggest new research directions that may originate from a synergistic blend of all the herein discussed topics. Finally, we discuss major challenges and open questions related to the application of SERS for understanding of chemical processes at the nanoscale, with special interest on *in situ* catalysts and biosensing.

Received 21st March 2017

DOI: 10.1039/c7cs00207f

[rsc.li/chem-soc-rev](http://rsc.li/chem-soc-rev)

### Key learning points

- It is essential to work in close vicinity to the surface, considering the short (<1 nm), and long (<3 nm) -range distance dependence of SERS.
- Capture agents can enable direct and indirect SERS sensing of non-metal-binding analytes.
- *Operando* SERS is a technique for monitoring chemical reactions at realistic conditions, promising for catalysis and industrial applications but still with challenges to overcome.
- Aluminum plasmonics allow for SERS in the UV, in this spectral range experimental considerations to minimize photodegradation are critical. UV-SERS might enable the detection of small and biological molecules not be attainable with visible-IR excitations.
- The importance of SERS substrate fabrication and functionalization in accordance with the final application to assure reproducibility and required robustness.

## 1. Introduction

SERS, regardless if understood as surface-enhanced Raman scattering or spectroscopy, is a well-established sensing technique and a field of research that is continuously evolving. This continued evolution can be attributed to the exquisite surface sensitivity of SERS, and has become explicitly linked to progression in nanomaterials engineering (design and fabrication). In SERS, the surface is used to boost the otherwise weak normal

Raman scattering (NRS) signal coming from analytes in close proximity to a plasmonic substrate.

Raman scattering refers to an inelastic light scattering process that provides a vibrational spectrum rich in chemical structure information. With typical Raman cross-sections on the order of  $10^{-30}$  cm<sup>2</sup> sr<sup>-1</sup> molecule<sup>-1</sup>, NRS from molecules is typically a very inefficient process.<sup>1</sup> In NRS, the intensity of Stokes scattering is proportional to the excitation power density and the Raman cross-section of the molecule. One method of enhancing the signal of NRS is to exploit electronic resonance effects. When the exciting laser energy falls within a molecular electronic transition (*i.e.* absorption band), Raman intensities can be  $10^2$  to  $10^6$  larger. This process is referred to as resonance Raman scattering (RRS) and can be interpreted as involving a larger molecular Raman cross-section.<sup>1,2</sup>

In SERS, Raman scattering signals are amplified by placing the molecule of interest in close vicinity to a metal surface of a

Department of Chemistry, Northwestern University, 2145 Sheridan Road, Evanston, Illinois 60208, USA. E-mail: fernanda.cardinal@northwestern.edu, emmavanderende2014@u.northwestern.edu, ryan.hackler@northwestern.edu, mcanally@u.northwestern.edu, pstair@northwestern.edu, schatz@northwestern.edu, vanduyne@northwestern.edu; Tel: +1-847-491-2952, +1-847-491-5266, +1-847-491-5657, +1-847-491-3516

plasmonic substrate; maintaining the above enumerated aspects of NRS: chemical information, laser power and molecular cross-section dependences.<sup>1</sup> SERS can be differentiated from many analytical sensing techniques by the rich vibrational spectroscopic information about an adsorbed molecule that it provides. This is one of the main reasons why it has been applied to a variety of fields, including electrochemistry, catalysis, biology, medicine, art conservation, materials science, and more. Another reason that SERS has been developed is that it can be combined with RRS (SERRS) to achieve single-molecule limits of detection, potentially elucidating information about chemical processes unobservable in ensemble measurements (those that represent the average signal of many individual molecules) (ref. 3 and references therein). Additionally, with proper instrumentation, sub-diffraction-limited resolution can be achieved and ultrafast study of molecular dynamics may be feasible. All these characteristics demonstrate that SERS, with a customized substrate, could answer fundamental chemical questions including reaction mechanisms (ref. 4 and references therein).

From fundamental and practical perspectives, it is important to understand the mechanisms by which the Raman scattering signal is boosted in SERS, as this helps guide what the expected limit of detection (LOD) can be for different analytes.<sup>1</sup> While there might not be universal consensus on the SERS mechanism within the scientific community, there is certainly unity in acknowledging that several factors have crucial roles in different limiting cases. Our adopted way of understanding SERS involves two proposed mechanisms: the electromagnetic (EM) and chemical (CHEM)

mechanisms (ref. 3 and 5 and references therein). The EM enhancement mechanism is directly related to the plasmonic properties of the substrate and hence to the dielectric function in combination with the nanostructures' composition, shape, size and local dielectric environment. Surface plasmon resonances localize and concentrate electromagnetic radiation augmenting the incident and emitted electric fields in the near-field region close to the surface. Hence, in SERS, the EM mechanism, or localized surface plasmon resonance (LSPR), amplifies both excitation and emitted radiation. Enhancement factors (EFs) of up to  $10^6$ – $10^8$  are attributed to the EM mechanism, which is typically considered the strongest source of signal amplification. The CHEM enhancement mechanism can also boost by up to  $\sim 10^2$  the Raman scattering process when the molecule is directly adsorbed to the metallic surface resulting in a charge-transfer that advantageously changes the molecule's polarizability.<sup>1,5b</sup>

These factors explain why, from a practical perspective, significant effort is focused on (1) engineering nanostructures with plasmonic metals (such as gold, silver and copper) and (2) bringing the molecule of interest within close proximity to take advantage of the enhancement mechanism (ref. 6 and references therein). Hot-spots are a particularly successful type of engineered features at the nano-scale, either as sharp objects or gaps which can produce SERS enhancements ranging from  $10^5$  to  $10^8$ . Importantly, the EM provided by hot-spots combined with RRS enhancement is by far the most frequent method to achieve single molecule sensitivity with SERS (ref. 3 and references therein). With such high sensitivity,



**From left to right: María Fernanda Cardinal, Emma Vander Ende, Ryan A. Hackler and Michael O. McAnally**

*Fernanda studied Chemistry (UBA, Argentina) and obtained a PhD degree advised by Prof. Luis M. Liz-Marzán and Prof. Jorge Pérez-Juste (2008–2012, University of Vigo, Spain). In 2012, she joined the Van Duyne Group at Northwestern University as a postdoctoral fellow. Her research focuses on novel plasmonic substrates for SERS and LSPR sensing. Recently, she has been appointed by the Nanosystems Institute (INS-UNSAM, Buenos Aires) as Associate Researcher and by CONICET. Emma is currently a 2015 NSF Graduate Fellow (NSF GRFP) and a PhD Candidate in Chemistry advised by Richard P. Van Duyne. She received her BS in Chemistry and BS in Biological Sciences with an emphasis on molecular biology and genetics from Northern Kentucky University in 2014. Her research focuses on the application of SERS to biosensing, statistical methods and CAESERS. Ryan received his BS degree in Chemistry and BA degree in Politics/Philosophy/Economics from Western Washington University in 2014. He is a graduate student co-advised by Peter C. Stair and Richard P. Van Duyne and his research focuses on using SERS to acquire structurally specific information about surface species present during ALD processes. Michael received his BS degree in Chemistry and Mathematics from the University of Wisconsin-Eau Claire in 2011, advised by Stephen Drucker. He is currently pursuing his graduate work on plasmonically-enhanced coherent Raman scattering jointly advised by Richard P. Van Duyne and George C. Schatz. His research combines both theoretical (DFT) and experimental studies.*

SERS may allow the detection of molecular changes upon adsorption; and therefore provide insight into surface science at the nanoscale.<sup>7</sup>

A common metric to quantify the signal amplification from surface enhancement in SERS is the EF, as it compares the surface-enhanced signal ( $I_{\text{SERS}}$ ) to the NRS signal ( $I_{\text{NRS}}$ ) normalized for the number of molecules probed (eqn (1))

$$\text{EF} = \frac{I_{\text{SERS}}/N_{\text{SERS}}}{I_{\text{NRS}}/N_{\text{NRS}}} \quad (1)$$

(ref. 1, 3, 4, 7 and 22 and references therein).

Typically,  $N_{\text{NRS}}$  is determined with the illuminated volume (requires spot size and depth of focus determination) in a solution of known concentration; and  $N_{\text{SERS}}$  is determined with the surface coverage of adsorbed molecule on the substrate for SERS and the illuminated area. Our preferred method for determination of surface coverage for electroactive adsorbates is cyclic voltammetry and/or double potential step chronocoulometry. EFs are meant to facilitate comparison between different SERS substrates and experimental approaches. However, direct comparison of EFs is non-trivial because (a) it is experimentally challenging to correctly quantify the surface coverage, and/or (b) in some cases maximum and in other cases average SERS EF or analytical EF are reported without clarification.<sup>1,4</sup> Unfortunately, underestimation of  $N_{\text{SERS}}$  results in overestimated EFs (ref. 1, 3, 4, 7 and 22 and references therein). Keeping these issues in mind, later in this tutorial review we suggest to report a lower limit average EF calculated from multiple spots or imaging scans rather than the maximum EF obtained at a single highly enhancing spot to provide a metric that is representative of the entire substrate. Hopefully this will help to minimize future discrepancies. We consider enhancement factor (EF) and limit of detection (LOD) as complementary metrics, if possible both should be reported. Later, we do not include the LOD as a tool for comparison of SERS substrates because from our perspective, LOD is more dependent on the collection efficiency of the Raman spectrometer utilized than EF. LOD is certainly a very useful figure of merit for quantitative SERS, and therefore we encourage its use for sensing applications.



**Peter C. Stair**

*Peter Stair received a BS in Chemistry from Stanford University in 1972 and a PhD from University of California, Berkeley in 1977 under the supervision of Gabor Somorjai. He has been on the faculty at Northwestern University since 1977. He is Professor of Chemistry, Chair of the Department, and Director of the Institute for Catalysis in Energy Processes. From 1997 to 2012 he was Director of the Center for Catalysis and Surface Science. He is also a Senior*

*Scientist in the Chemical Sciences and Engineering Division at Argonne National Laboratory and was Deputy Director of the Institute for Atom-efficient Chemical Transformations. His research interests are in the synthesis, characterization, and physical properties of heterogeneous catalysts. He has worked in surface science and in situ Raman spectroscopy. His goal is to develop fundamental understanding in catalysis science that leads to advances in industrial chemistry and energy technology.*



**George C. Schatz**

*George C. Schatz is the Morrison Professor of Chemistry at Northwestern University. He received his undergraduate degree at Clarkson University and PhD at Caltech. He was a postdoc at MIT, and has been at Northwestern since 1976. Schatz is a member of the National Academy of Sciences, the American Academy of Arts and Sciences, and he has been Editor-in-Chief of the Journal of Physical Chemistry since 2005. Schatz is a theoretician specializing in*

*electronic structure methods, electrodynamics, and statistical mechanics, who studies the optical, structural and thermal properties of nanomaterials, including plasmonic nanoparticles, SERS, DNA and peptide self-assembled nanostructures, and carbon-based materials, with applications in chemical and biological sensing, electronic and biological materials, and solar energy.*



**Richard P. Van Duyne**

*Prof. Van Duyne is the Charles E. and Emma H. Morrison Professor of Chemistry and of Biomedical Engineering at Northwestern University. He received a BS (1967) at Rensselaer Polytechnic Institute and PhD (1971) at the University of North Carolina, Chapel Hill, both in Chemistry. He is a member of the National Academy of Sciences and the American Academy of Arts and Sciences. He is known for the discovery of surface-enhanced*

*Raman spectroscopy (SERS), the invention of nanosphere lithography (NSL), and the development of ultrasensitive nanosensors based on localized surface plasmon resonance (LSPR) spectroscopy.*



In this tutorial review, we focus on a few recent advances in fundamental and applied aspects of SERS that may lead to significant chemical applications. This progress is either related to the quality of the plasmonic substrate or the molecule localization to the substrate. The advances were chosen because we believe a combination of them could lead to exciting future research. In the next section, we discuss SERS distance dependence and *operando* SERS to understand how far from the surface SERS can probe, an important consideration for successfully monitoring catalytic reactions. Later, in Section 3, we direct our attention to the SERS substrate, focusing on aluminum as a UV plasmonic material as well as a brief enumeration of suggested practices that might facilitate reproducible SERS spectra across different research groups. We then review short-distance capture strategies for increased selectivity and adsorption efficiency in Section 4, with a focus on direct sensing schemes over indirect ones. Lastly, we discuss remaining challenges and possible new directions that could arise from the synergistic combination of all the herein discussed topics, which we foresee could provide understanding of chemical processes and expansion of SERS applications.

## 2. SERS distance dependence and *operando* SERS

Performing *operando* experiments requires measurements to be made under temperatures and pressures pertinent to the reaction. For SERS to be a viable technique in applications such as molecular sensing and *operando* measurements involving catalytic reactions, the variation in SERS intensity resulting from the distance between the enhancing surface and the analyte molecule must be taken into account. This variation in intensity is predominantly the result of the EM enhancement mechanism, which does not require the analyte to be in direct contact with the plasmonic surface. The EM mechanism does, however, require the molecule to be within a few nanometers from the surface for an appreciable enhancement to be obtained.

The distance dependence of SERS has been investigated in the past, both in theory and in experiment. Gersten and Nitzan<sup>8</sup> first developed a model to describe the decay of SERS signal as a function of molecule-metal distance for various metals (Ag, Cu, Au) and spheroidal shapes. Later, various experimental groups used a number of molecular probes and spacers to evaluate the SERS signal decay and how it compared with the Gersten and Nitzan model. Using a simplified sphere model and  $E^4$  approximation the model can be written as:

$$I = \left(1 + \frac{r}{a}\right)^{-10} \quad (2)$$

where  $I$  is the SERS intensity,  $a$  is the radius of curvature of the field enhancing nanostructure, and  $r$  is the distance between the analyte and plasmonic surface. One of the earliest efforts into experimentally evaluating SERS signal decay by Kovacs *et al.*<sup>9</sup> used Langmuir-Blodgett spacer layers of arachidic acid and a monolayer of tetra-*t*-butyl phthalocyanine as the probe molecule.

Other researchers utilized various self-assembled monolayers (SAMs) of thiols where the thiol acted as either the spacer layer exclusively, or as both the spacer layer and probe molecule. SAMs have shown fewer structural defects in the film than Langmuir-Blodgett spacer layers, and thus are a more reliable and reproducible spacer layer. Ye *et al.*<sup>10</sup> functionalized the end of the SAMs with an azobenzene moiety for the molecular probe. Compagnini *et al.*<sup>11</sup> simply used alkanethiols of various alkane chain sizes, in which the terminal methyl vibrations served as the probe. Kennedy *et al.*<sup>12</sup> used alkanethiols only as the spacer layer, and benzene and *t*-butylbenzene as probe molecules. Tian *et al.* established the long-range distance dependence associated shell-isolated nanoparticle-enhanced Raman spectroscopy (SHINERS), with decent agreement with finite-difference time-domain calculations of a shell-isolated nanoparticle array.<sup>13</sup> However, inconsistency in either EFs or a failure to address deviations from the Gersten and Nitzan model remained a problem throughout these studies. It was only recently when our group used atomic layer deposition (ALD) to deposit thin metal oxide films on a single substrate that the EF inconsistency was finally overcome, while at the same time acquiring angstrom-scale resolution of the spacer layer.<sup>5a</sup> In this study, we were able to resolve short- and long-range components in the Gersten and Nitzan model by using a single Ag film-over-nanospheres (Ag FON) substrate throughout the course of an ALD of aluminum oxide, using the methyl-alumina surface species as the probe molecule. As illustrated in Fig. 1, we used two different vibrational modes (sym. C-H and sym. Al-CH<sub>3</sub> stretches) to monitor the decay of SERS signal with respect to the spacer layer. Experimentally, the Gersten and Nitzan model (eqn (2)) failed to fit our data, so we used a two-term phenomenological expression (see eqn (3)). In this modified Gersten and Nitzan model (eqn (3)),  $a_1$  and  $a_2$  are the short- and long-range radii of curvature of features, respectively. The different radii of curvature are the result of small (<1 nm) and large (>10 nm) nanoparticle structures associated with the heterogeneous Ag FON surface (see SEM micrograph in Masango *et al.*<sup>5</sup>).

Thus, our results suggest that SERS distance dependence is conditioned by the substrate nanostructure, and should be contemplated for sensing applications. In particular, for *operando* SERS measurements where the distance between the analyte and the substrate might vary and heterogeneous nanostructures with high EF are typically necessary, to anticipate the decay of the SERS signal from a given substrate is certainly important.

$$I_{\text{SERS}} = C_1 \left(1 + \frac{r}{a_1}\right)^{-10} + C_2 \left(1 + \frac{r}{a_2}\right)^{-10} \quad (3)$$

*Operando* spectroscopy simultaneously studies fundamental spectroscopic characterization of surface phenomenon and catalytic performance.<sup>14</sup> *Operando* measurements differ from *in situ* measurements by being performed under “true catalytic” conditions, where catalytic activity/selectivity measurements can be made alongside structural measurements.<sup>14</sup> *In situ* SERS typically falls short of providing insight into the catalytic system

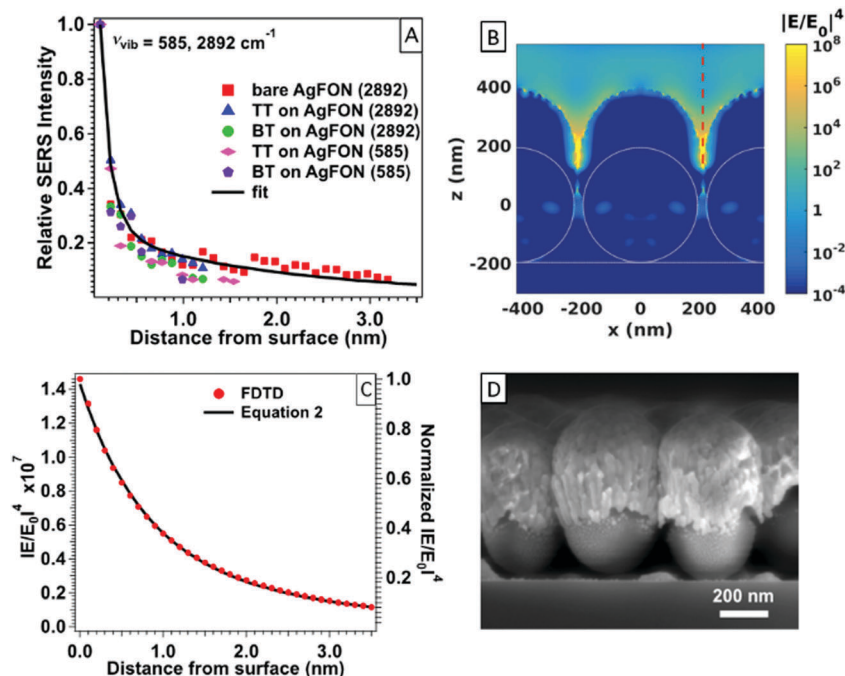


Fig. 1 Distance dependence of SERS. (A) SERS intensity decay of sym. C–H ( $2892\text{ cm}^{-1}$ ) and sym. Al–CH<sub>3</sub> ( $585\text{ cm}^{-1}$ ) stretches as a function of distance with a two-term fit (eqn (2)). (B) Spatial distribution of local electric field enhancement from FDTD calculations of simulated Ag FON surface. (C) Near-field distance dependence profile at gap of simulated Ag FON surface observed at the dashed red line in (B). (D) Side-view SEM micrograph of Ag FON substrate used. Reprinted and adapted with permission from ref. 5a. Copyright 2016 American Chemical Society.

of interest due to either the cell or the substrate being incapable of withstanding the high pressures and temperatures necessary for measuring relevant kinetic information. Issues such as heat and mass transfer gradients can also arise from cell design and can complicate kinetics measurements. Over other techniques, *operando* SERS has the advantage of being able to probe the lower wavenumber region during reaction-specific conditions as a means of acquiring structurally relevant information about the analyte species. By probing the low wavenumber region, where pertinent metal–carbon and metal–oxygen vibrations are located, one can determine the structures of transient species present during the reaction. This type of study was recently performed on the alumina ALD process to show previously unestablished transient dimeric surface species.<sup>5b</sup> Illustrated in Fig. 2 are the low wavenumber vibrational modes that we used to make structural determinations about the methylalumina species. These measurements were performed in the ALD reactor at  $70\text{ }^{\circ}\text{C}$ .

The largest obstacle in utilizing *operando* SERS is the requirement that the reaction take place within a few nanometers from the plasmonic surface. If the catalytic reaction does not involve the plasmonic surface as the catalyst, then the whole catalytic system (*i.e.* the catalyst, reagents, and inert separation layer between the catalyst and plasmonic surface) must be incorporated near the surface in a way that optimizes the Raman signal during the experiment. Because a multitude of factors inherent to the catalytic reaction (not limited to the coverage, lifetime, and Raman scattering cross-section of analyte species) will limit the SERS signal, the total distance

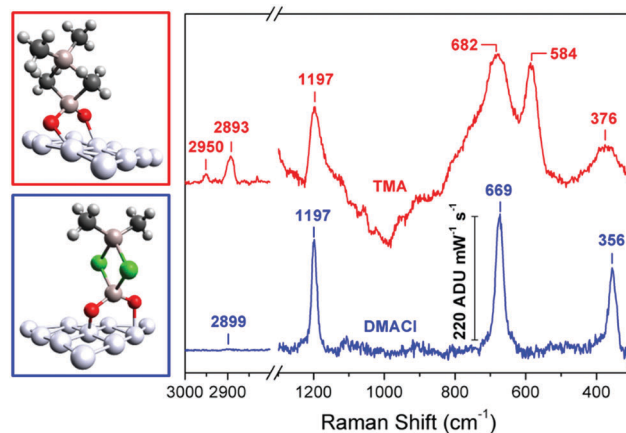


Fig. 2 Structural determination of surface species. Left: Molecular structures of transient dimeric surface species. Right: SERS difference spectra of Ag FON exposed to 60 s of TMA (1st cycle) (red) and 60 s of DMACI (1st cycle) (blue) in the low wavenumber ( $1300\text{--}300\text{ cm}^{-1}$ ) and C–H ( $3000\text{--}2800\text{ cm}^{-1}$ ) stretching regions. Three peaks are observed with both precursors: at  $1197\text{ cm}^{-1}$  (symm.  $\nu(\text{Al-C})$ ,  $\delta(\text{CH}_3)$ ), at  $682/669\text{ cm}^{-1}$  ( $\nu(\text{C-H})_{\text{rocking}}$ ), and at  $376/356\text{ cm}^{-1}$  (symm.  $\nu(\text{Al-bridge})/\delta(\text{Al-bridge})$ ) and we attribute the peaks at  $1197$  and  $682/669\text{ cm}^{-1}$  to alumina surface species with a coordinated methyl group. The peak seen only in the TMA spectrum at  $584\text{ cm}^{-1}$  ( $\nu(\text{bridged C-H rocking})$ ), we assign to the bridged methyl rocking in the parallel and perpendicular dimer models based on comparison to simulations. Reprinted with permission from ref. 5b. Copyright 2017 American Chemical Society.

between the analyte and plasmonic surface must be minimized to obtain appreciable signal.

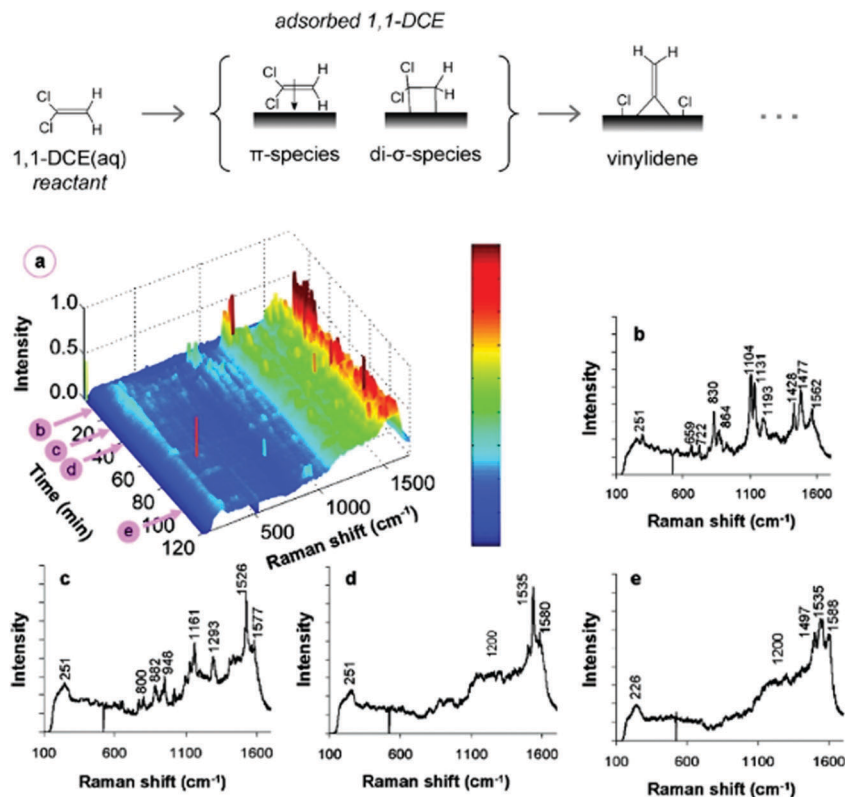


Fig. 3 *In situ* SERS of hydrodechlorination reaction. Top: Scheme of some proposed surface intermediates. Bottom: (a) Waterfall plot of time-resolved spectra acquired from the reaction of 1,1-dichloroethene (DCE) and hydrogen on Pd/Au nanoshells; and individual spectra at 12, 30, 41, and 100 min (b, c, d and e, respectively) after reactants injection. Here we do not intend to do extensive peak assignments to  $\pi$ -bound and di- $\sigma$ -bound DCE but to illustrate the information achievable with *in situ* SERS. For example, the 250 cm<sup>-1</sup> peak, corresponding to metal–chlorine vibrations, was observed to increase then decrease over the course of the reaction. The authors hypothesized desorption by the formation of HCl. Dechlorination is also supported by the disappearance of the peaks in the 600–900 cm<sup>-1</sup> range, where carbon–chlorine vibrational modes are expected. Also, the appearance of modes near 954, 1160, and 1430 cm<sup>-1</sup> could be indicative of di- $\sigma$ -bound 1,1-DCE onto the surface. Overall, this figure exemplifies the power of *in situ* SERS for monitoring structural changes of surface species in a dynamic way. Reprinted and adapted with permission from ref. 17. Copyright 2008 American Chemical Society.

Most efforts into *operando* SERS for heterogeneous catalysis have either involved using a specific, sufficiently strong Raman scatterer with limited industrial or catalytic significance or have used the plasmonic surface as both the field enhancing substrate and catalyst. The Weaver group examined the adsorption of gases (NO, CO, and O<sub>2</sub>) at various temperatures (25–200 °C)<sup>15</sup> and the electrocatalysis of small molecules<sup>16</sup> on transition metals (Pt, Pd, Rh, Ru), laying the foundation for probing relevant heterogeneous reactions outside the conventional plasmonic metals (Au, Ag). Later, Heck *et al.* studied the catalytic hydrodechlorination of 1,1-dichloroethene (1,1-DCE) in water (at room temperature) using SERS on Au nanoshells decorated with Pd islands (see Fig. 3).<sup>17</sup> In their experiments, Heck *et al.* identified vibrational modes associated with the adsorption and binding behavior of the reactant and intermediates, and monitored how they changed with reaction time. When performing the hydrodechlorination reaction in a solution of 1,1-DCE and hydrogen, the H<sub>2</sub> was postulated to dissociatively adsorb onto the surface and accelerate the dechlorination, based on the appearance of broad bands around 250 cm<sup>-1</sup> (metal–chlorine and metal–carbon vibrational modes)

after only 5 minutes (Fig. 3b). In contrast, these bands did not appear in the hydrogen-absent experiment until 20 minutes. Vinyl surface species were also suspected of being present based on small modes at ~1230, ~1360, and ~1580 cm<sup>-1</sup>, although these are much harder to pick out. There were modes that appeared at ~954, ~1160, and ~1430 cm<sup>-1</sup>, indicative of di- $\sigma$ -bound 1,1-DCE on the surface (Fig. 3b and c).  $\pi$ -Bound 1,1-DCE was also observed based on additional peaks in the 1000–1100, 1220–1290, and 1500–1600 cm<sup>-1</sup> regions. Peaks in the 600–900 cm<sup>-1</sup> region (C–Cl stretches) suggested partially dechlorinated 1,1-DCE surface species, as these modes were not present in the hydrogen-absent experiment. By the end of the experimental run (100 minutes long), peaks in the 250 and the 600–900 cm<sup>-1</sup> regions decreased in intensity, suggesting complete dechlorination of surface species. Broad spectral bands from 1200–1600 cm<sup>-1</sup> suggested adsorbed vinylidene species that persisted throughout the experiment (Fig. 3d and e).

Unfortunately, the instability of plasmonic substrates to conditions of high temperatures (>200 °C) and pressures ( $\geq 1$  atm) has prevented *operando* measurements on relevant catalytic systems. It is thus desirable to make highly enhancing

substrates more chemically and thermally robust to support such conditions.<sup>18</sup> In terms of thermal stability, the architecture of the plasmonic substrates must be maintained during relevant temperatures in order to avoid annealing and thus degradation of the EM field enhancement. Work by Whitney *et al.*, for example, has shown that thin overcoats of alumina prepared *via* ALD onto periodic particle arrays of Ag were sufficient to stabilize the particles and minimize their reshaping at temperatures up to 500 °C.<sup>19</sup> Overcoats of the plasmonic material by metal oxides may also serve as a chemically inert barrier, but considerations into the thickness of the overcoat must be made such that the SERS signal is optimized, as previously mentioned.

Another problem that is pervasive in SERS applications is the reproducibility in field enhancement from substrate to substrate. The variation in field enhancement across substrates is a consequence of the variability in nanostructures and reproducibility of the production method. A lack of field enhancement uniformity makes quantitative comparisons for catalytic reactions difficult. In the case of Ag FONs, reproducibility has been optimized to the point where variation in EFs across a single substrate (*i.e.* different spots) and across multiple substrates has been reduced to <10%.<sup>20</sup> For other substrates missing EFs uniformity, standards are often used to account for fluctuations in intensity resulting from hot-spot variability.<sup>21</sup> For example, Weathersson *et al.* used covalently bound 4-nitrothiophenol as an internal standard during SERS monitoring of the aldol condensation of 4-(methylthio) benzaldehyde with free acetone. The use of nitrothiophenol internal standard was appropriate because it binds in a similar manner to the gold surface as the analyte of interest. Because of the reproducibility problems associated with some SERS substrates, an internal standard should always be used if possible. One should be aware, however, that the internal standard should not interfere with the catalytic reaction and analyte, and that the internal standard should have similar affinity to the surface, and be used at a relatively low concentration compared to the analyte.

In moving forward with applying SERS towards *operando* monitoring of catalytic reactions as a means of acquiring structure–function relationships, several considerations must be made for each unique system. Depending on the temperatures and pressures of the system, and the Raman scattering cross-section of the reactants and products, different preparations of the substrate and catalyst must be pursued. As discussed, making the substrate resistant to chemically relevant conditions is necessary, which requires an inert layer between the plasmonic substrate and the catalyst. However, the inert layer introduces a certain amount of distance between the SERS substrate and the analyte, which results in a decreased SERS signal. Depending on the analyte, this extra surface separation can pose a challenge in measuring vibrational modes. Still, recent efforts in making thin inert separating layers and robust reproducible SERS substrates may lead to viable studies of more interesting catalytic systems. We consider that metal oxides (such as Al<sub>2</sub>O<sub>3</sub>, TiO<sub>2</sub>, and SiO<sub>2</sub>) would prove to be the

most useful protection layers due to their thermally and chemically inert properties. Finally, we note that plasmon-driven catalysis and hot-electrons as reducing agent are actively discussed in literature as they might lead to new technologies.<sup>22</sup>

### 3. Alternatives to gold and silver as plasmonic materials: aluminum for deep UV-SERRS

SERS spectra are most commonly acquired with laser excitation sources in the visible-NIR range of the electromagnetic spectrum. Even though UV Raman spectroscopy is a well-established field of research, the surface-enhanced version, UV-SE(R)RS is not. In this section we address the developmental hindrances to UV-SERRS, distinct advantages of UV-SERRS over visible-NIR SERS, research efforts that utilize aluminum as an alternative plasmonic substrate for UV excitation wavelengths, and experimental challenges and considerations relevant for SERS measurements in the UV and visible-NIR.

We attribute the slow pace of UV-SERRS advances to three main factors: first, UV spectroscopy requires customized instrumentation for the UV range, which typically increases cost and initially was not cross-compatible with visible-NIR optimized equipment. Fortunately, thanks to continual improvements in UV protective coatings for optics, CCD cameras sensors, spectrographs and lasers designs, it is now possible to purchase commercial UV-vis-NIR compatible (though not simultaneously optimal) Raman spectrometers or to build UV-devoted home-made set-ups of high performance (higher spectral resolution and signal-to-noise ratio). Hence, instrumental limitations are no longer significant obstacles. Second, early theoretical predictions based only on the EM field enhancement calculations at UV wavelengths illustrated poor plasmonic properties for Au and Ag, which are the most widely used metals for SERS substrates fabrication. In the UV, the surface plasmon resonances of Au, Ag and Cu are overwhelmed by interband transitions; suggesting the need to switch to alternative materials and to optimize fabrication methods for UV plasmonic SERS substrates (ref. 23 references therein). A third deterrent and probably the most frequent one to UV-SERRS development is photodegradation of adsorbates. It is experimentally challenging to avoid photodamage of the adsorbate by the UV excitation light source,<sup>7</sup> this constitutes the main disadvantage for UV over visible SERS applications.

Distinct advantages of UV-SERRS over visible and NIR SERS are increased Raman scattering efficiency because Raman intensity varies with the fourth power of the observed frequency ( $\nu^4$ ), additional signal enhancement due to electronic resonance effects if the excitation laser wavelength is close to absorption bands of the adsorbate molecule, higher spatial resolution due to the direct dependence with wavelength of diffraction-limited imaging, and (below 250 nm) bypassing fluorescence backgrounds.<sup>1,2,23,24</sup> These advantages position UV-SERRS as a technique that might complement visible-NIR SERS for studying biologically- and catalytically-relevant adsorbates. Fortunately, the vast majority



of biomolecules (e.g., amino acids, proteins, steroids) and small molecules have electronic transitions with absorption in the deep UV (190–300 nm) that can be exploited for resonance Raman scattering (RRS). In fact, tuning the excitation laser for UV-RRS enabled selective enhancement of particular vibrations in specific regions of the macromolecule myoglobin,<sup>2b</sup> suggesting that an extension to UV-SERRS might be suitable to monitor structural changes of proteins on metallic nanoparticles. Also, this increase in the Raman cross-section due to RRS might be exploited to study catalytic or photoinduced reactions such as photodissociation of methyl iodide, photopolymerization of stilbenes among many others.<sup>2a,24b,25</sup>

In the UV-SERRS literature, metals such as Au, Ag, Au–Ag, Au–Pd, Au–Pt, Pd, Pt, Rh, Cu, Ga, In, and Co have been studied experimentally as plasmonic substrates.<sup>26</sup> The pioneering UV-SERS work by the Tian group on thiocyanate anion detection on Ru, Rh, Pd and Pt roughened electrodes,<sup>26a,b</sup> together with previous RRS investigations (ref. 2 and references therein) suggest that UV-SERRS is suited to study surface species during electrochemical or catalytic reactions on metals for which the surface enhancement is higher in this spectral region due to their dielectric functions.

During the last decade there has been significant progress in the fabrication of aluminum nanostructured substrates with acceptable enhancement, despite the presence of its native oxide layer at ambient conditions that reduces EM field enhancement. To the best of our knowledge, this progress enabled the first comparison of adenine UV-SERS spectra on various nanostructures constituted of the same metal and comparison to silver substrates. Here, we will focus on aluminum with the intention to encourage further optimization of UV-SERS substrates. We also note that although the plasmon width is typically larger for Al than Ag, the physical origin of the broadening is due to radiative effects rather than electron-phonon interactions (ref. 27 and references therein), so there is the opportunity to manipulate the lineshape for Al by varying particle shape and arrangement to produce narrower plasmons.<sup>27</sup> We believe that with design optimization, Al substrates might have superior or, at least, comparable performance at UV to Ag and Au.

In Fig. 4 we illustrate various types of aluminum nanostructures that have been studied: an array of Al disks utilized by Jha *et al.* to detect UV-SERRS spectra from an adenine film<sup>28</sup> (Fig. 4A); arrays of Al nanovoids prepared directly by colloidal lithography<sup>25</sup> (Fig. 4B) and indirectly with a re-usable nanoimprinting colloidal stamp<sup>29</sup> both utilized for UV SERRS detection of adenine from solutions; Al FON (Fig. 4C) utilized for UV-SERRS detection of multiple molecules;<sup>23</sup> and nanostructured films utilized for the UV-SERRS detections of crystal violet prepared by sputtering<sup>7</sup> and by laser-direct-writing<sup>30</sup> (Fig. 4D).

For the aluminum substrates mentioned, we focus here on our achievements with Al FONs. General characteristics of FON substrates are: easy and low cost fabrication, tunable localized surface plasmon resonance (LSPR) according to the size of the packed spheres, strong EM field enhancement and reproducible performance for SERS sensing. Exploiting these characteristics, we prepared FONs with two different spheres sizes, 170 and

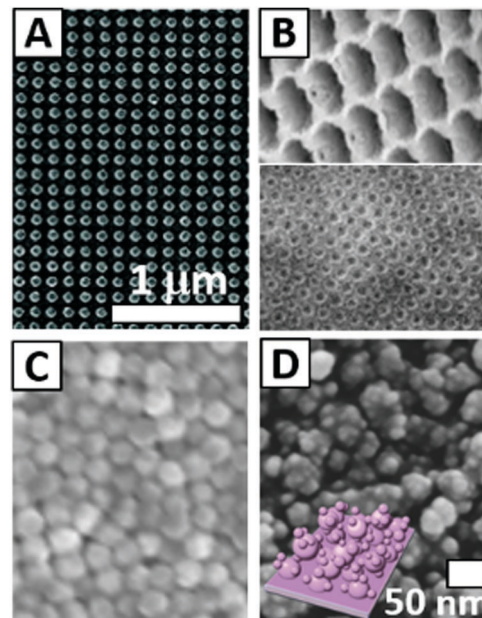


**Fig. 4** Aluminum substrates used for UV-SERRS. (A) Al nanoparticle array. (B) Al nanovoids array prepared by tape stripping (top) and nanoimprint (bottom). (C) Al film-over-nanospheres. (D) hot-spots rich Al nanostructured film. For (A–C) Scale bar 1  $\mu\text{m}$ . For (D) scale bar 50 nm. Reprinted and adapted with permissions from (A) (ref. 28) (B) top: (ref. 25) bottom: (ref. 29) (C) (ref. 23) (D) (ref. 30). Copyright 2012, 2013, 2014, 2016, American Chemical Society. Copyright 2017 John Wiley & Sons, Ltd.

210 nm, which generated LSPRs at 222 and 309 nm for Al FONs and 368 and 400 nm for Ag FONs, respectively. We investigated their UV-SERS performance with four different adsorbates (adenine,  $\text{Ru}(\text{bpy})_3^{2+}$ , mercaptohexanol and *trans*-1,2-bis(4-pyridyl)-ethylene, BPE) by deep UV excitation. In Fig. 5 we present UV-SERRS spectra of two adsorbates only: adenine and BPE. This simplifies the discussion by comparing two standard SERS analytes and demonstrates the substrates' performance for the most commonly used biomolecule probed in the UV (adenine). For UV-SE(R)RS spectra of  $\text{Ru}(\text{bpy})_3^{2+}$ , mercaptohexanol and further discussion we refer the readership to ref. 23. In our experiments, we incubated Al and Ag FONs as well as Al and Ag mirrors in 1 mM solutions of the target analytes and later rinsed them to minimize the number of un-bound molecules. At our excitation wavelength, 229 nm, both adenine and BPE are resonant adsorbates. In an attempt to differentiate and quantify the enhancement generated by the nanostructured plasmonic surface from the enhancement provided by the electronic resonance effect, we compare FONs and mirrors. We attribute the enhancement observed with mirrors (green traces) to normal resonance Raman contributions, and total enhancement on FONs substrates (blue and red traces) to a combination of surface enhancement and resonance Raman effect. In the case of BPE, it appears that resonance effects are not large. On Ag and Al mirrors and 170 nm FONs, we see almost negligible enhancement of BPE vibrational modes compared to the intense spectra acquired on Ag and Al FONs (blue traces) generated using 210 nm spheres size. For adenine, the resonance



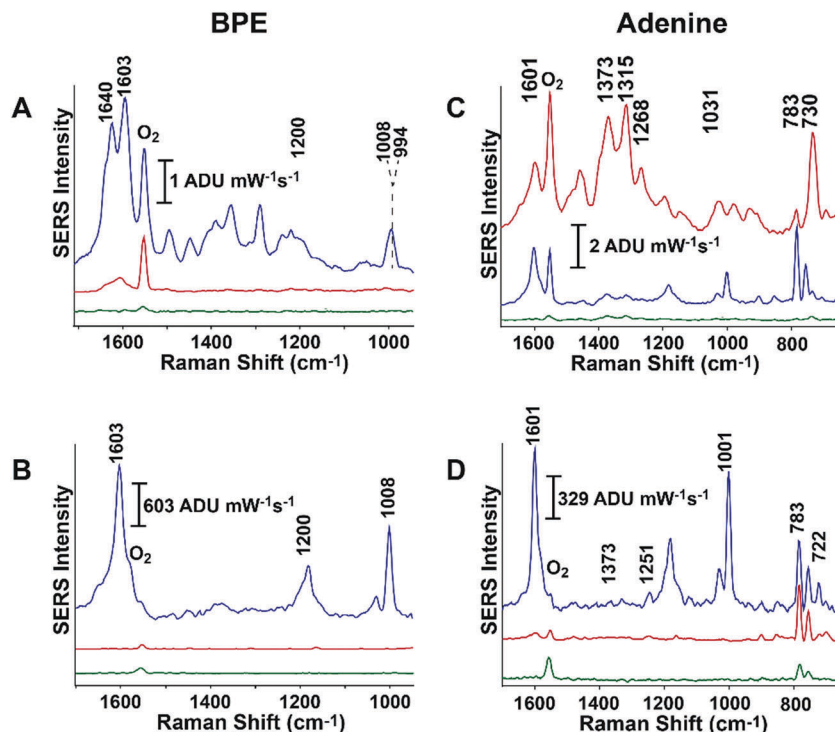


Fig. 5 BPE and Adenine resonance Raman spectra on Al and Ag substrates. All spectra were acquired with 229 nm excitation. Upper row corresponds to silver (A and C) and lower row to aluminum (B and D). Raman spectra acquired on FONs prepared with 170 nm spheres size are shown in red, 210 nm sphere size in blue, and mirror substrates in green traces. Peaks labeled with O<sub>2</sub> represent the position of the atmospheric oxygen peak ( $\sim 1555\text{ cm}^{-1}$ ), other peak assignments correspond to the literature values of the adsorbates. Highest SERS spectral intensities and signal-to-noise ratio are observed with Al FONs prepared with 210 nm spheres ( $\lambda_{\text{exc.}} = 229\text{ nm}$ , spectra normalized to atmospheric N<sub>2</sub> vibration at  $2332\text{ cm}^{-1}$ ). Reprinted and adapted with permission from ref. 23. Copyright 2016 American Chemical Society.

enhancement is more evident and characteristic spectral features of adenine are clearly observed on both Ag and Al mirrors. Nevertheless, Al FON (210 nm, blue) and Ag FON (170 nm, red) provide much higher enhancement than the mirrors; hence demonstrating that nanostructuring adds signal amplification on top of the resonance effect and the multiplicative effect of resonance Raman with the EM enhancement in SERRS. For both analytes, adenine and BPE, the highest SERS signal intensities were achieved with Al rather than Ag (see scale bars). Experimentally, in our results there is no correlation between the substrate LSPR and the total UV-SERS signal enhancement. Consequently, we caution that in the UV, optimal enhancement cannot be predicted solely on sphere size and LSPR wavelength. Overall, we found that Al FONs with a native Al<sub>2</sub>O<sub>3</sub> oxide layer have plasmonic properties for deep UV-SERRS that in combination with the resonance enhancement of the adsorbates themselves can give average enhancement factors of the order of  $10^6$ , broadening the SERS application range.<sup>23</sup>

For future expansion of UV-SERRS with chemical applications, other experimental obstacles should be considered besides the challenge of fabricating satisfactory substrates. A problem common to all UV-SERRS reports cited herein is photodegradation of the adsorbate molecule by UV radiation. In some cases, this was avoided by working in solution phase;<sup>25,26a,28,29</sup> in other cases, photodegradation was minimized by using low excitation power.

From our perspective, photodamage may be circumvented by working at low enough power densities ( $\sim 5\text{ mW cm}^{-2}$ ) and

short acquisition times ( $\leq 30\text{ s}$ ) in stirred solution; conditions that are compatible with biological, electrochemical and catalytic experiments. In this context, it will be extremely valuable if researchers share detailed experimental conditions and sequential spectra acquisitions (in normalized units, counts  $\text{mW}^{-1}\text{ s}^{-1}$ ) to evaluate the extent of photodamage. We also noticed in recent literature a shortage of comparisons between nanostructured and flat substrates of the metal under study; and to other standard metals such as gold and silver, limited adsorbate variety, and incubation procedures that could cause adsorbate crystallization and consequently normal Raman acquisition instead of SERS. In Fig. 6, we detail what we believe are good practices to facilitate reproducible SERS data and thorough SERS substrate characterization. By sharing with the readership the way we critically think through these basic experimental aspects, we hope to guide the expansion of SERS chemical applications at all spectral ranges in a reproducible manner.

#### 4. Short-distance capture strategies for capture agent-enabled SERS (CAESERS)

In Section 2 of this tutorial review, we demonstrated that the highest surface enhancement of the SERS signal is experienced

Aspects to consider for	
Substrate Characterization	Reproducible SERS spectra
<ul style="list-style-type: none"> <li>• Characterize the optical properties (LSPR)</li> <li>• Quantify surface coverage to calculate EFs</li> <li>• Calculate and report lower limit average EFs, not maximum EFs for the EFs</li> <li>• Measure several adsorbates (resonant and non-resonant)</li> <li>• Verify that the surface spectra are shifted by <math>\sim 1\text{--}25\text{ cm}^{-1}</math> in comparison to the bulk solution spectra</li> <li>• Compare experimental data to theoretically calculated spectra.</li> <li>• Perform sequential acquisitions, evaluate if the analyte is photodegrading.</li> <li>• Calculate EFs with several peaks at different acquisition time points</li> <li>• Compare SER(R)S spectra on substrate of interest to that of a flat mirror and that of analyte normal Raman in solution or solid phase</li> </ul>	Reproducible adsorption of molecules: <ul style="list-style-type: none"> <li>• Substrate incubation</li> <li>• Spin coating</li> <li>• Drop casting</li> </ul> followed by rinsing to avoid analyte crystallization <ul style="list-style-type: none"> <li>• Average across the substrate and check for reproducibility: If possible perform Raman imaging, if not measure at least 3 different spots of the substrate, in at least 3 different substrate fabrication batches, and on at least 3 different experimental acquisition days</li> <li>• Provide in publications the spectra acquisition details (type of spectrometer used, micro or macro Raman, type of objective used; dry or wet conditions, ambient; power, and acquisition time)</li> <li>• Provide in publications data analysis details (baseline subtraction, normalization, smoothing, fittings or chemometric related considerations)</li> <li>• Spectral modeling: provide details of software, theoretical methods, simulation parameters, and final molecular system structures used</li> </ul>

Fig. 6 Suggested practical aspects to facilitate SERS spectra reproducibility across different laboratories (ref. 1, 6 and 23 and references therein).

within 1 nm of the surface of the plasmonic enhancing SERS substrate.<sup>5a</sup> Therefore, in an ideal situation, the analyte to be probed by SERS is in direct contact with the substrate, minimizing the distance to the substrate and maximizing the SERS signal intensity. Molecules that exhibit a high affinity for plasmonic metals are primarily those with thiol (which form covalent metal–S bonds), amine, cyanide, and carboxylic acid functional groups; and their adsorption depends on solution pH and ionic strength, steric hindrance around the affinity group, and the surface coverage and charge of the SERS substrate.<sup>31</sup> Since SERS presents several analytical advantages (high sensitivity, label-free detection, rich chemical information), it is desirable to widen the scope of detectable analytes beyond those that directly bind to metal surfaces. To do so, strategies are required that either (1) capture non-metal-affinitive molecules within the SERS sensing volume ( $<2\text{ nm}$  from the surface),<sup>5a</sup> enabling direct detection of the molecule, or (2) utilize a scheme whereby the presence of the analyte molecule is indirectly detected.

There are many strategies for what we refer to here as capture agent-enabled SERS (CAESERS) that have been developed in recent years, ranging from cross-coupling with metal-affinitive ligands,<sup>32</sup> SAMs of thiolated molecules,<sup>33</sup> polymer coatings, molecular recognition agents,<sup>34</sup> aptamers,<sup>35</sup> and antibody fragments.<sup>36</sup>

In this section, we focus on generalized strategies for CAESERS that (i) are applicable to a wide range of analytes (not specific to single analytes as are aptamers and antibodies), and (ii) employ capture agents that are short in length, to maximize the surface enhancement effect. Specifically, we review recent advances in directly tethering molecules to metal nanostructures *via* cross-coupling reactions, and capturing

molecules with low molecular weight SAMs and “cage-like” molecular recognition agents such as cucurbit[*n*]urils, calix[*n*]arenes, and cyclodextrins.

#### 4.1 Direct tethering *via* cross-coupling reactions

The most straightforward approach to bringing a molecule close to the surface of a SERS substrate is to directly tether the molecule to the surface by cross-coupling it with a short metal-affinitive “linker” molecule. There are many cross-coupling reactions that have accomplished this, including Diels–Alder reactions,<sup>32a</sup> carbodiimide coupling,<sup>32b</sup> and reactions that fall under the umbrella of “click” chemistry (ref. 37 and references therein). However, the latter has mainly been used to conjugate Raman reporters (also called “tags” or “probes”, those are molecules with high Raman cross-sections) to the molecule of interest. This enables indirect sensing of the molecule of interest; the detection of the Raman reporter implicates the presence of the molecule of interest. Of the former coupling reactions, we focus here on carbodiimide coupling. The linker in a carbodiimide coupling reaction can be short in length ( $<0.5\text{ nm}$ ), minimizing the distance between the molecule of interest and the SERS substrate surface, which enables direct sensing of the molecule of interest. The linker can also be thiolated, lending the stability of a covalent S–metal bond to the sensing system.

A particular type of carbodiimide cross-linking, 1-ethyl-3-(3-dimethylaminopropyl)carbodiimide (EDC) coupling, has been successfully used to tether molecules to plasmonic metal nanostructures for SERS. EDC forms an *o*-acylisourea active ester from a carboxylic acid, which then reacts with *N*-hydroxy-sulfosuccinimide sodium salt (NHS) to form a reactive ester intermediate. This intermediate reacts with a primary amine to form an amide bond. Thus, EDC coupling can be used to link

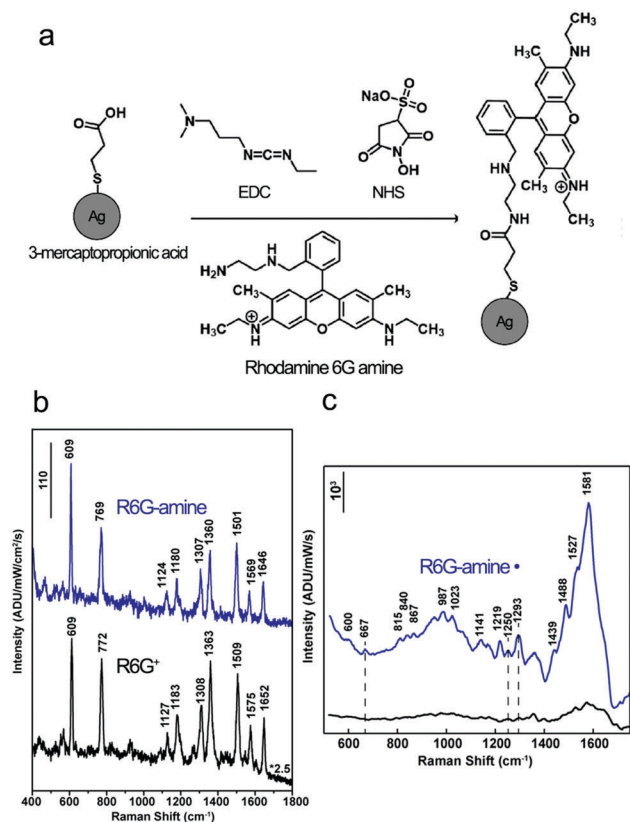


Fig. 7 SERS of R6G-amine assisted by carbodiimide cross-coupling. (a) Schematic illustrating the conjugation of R6G-amine to 3-mercaptopropionic acid-functionalized Ag nanoparticles by EDC coupling. (b) SERS spectra of physisorbed R6G<sup>+</sup> (black trace, 2.5× intensity) and EDC-coupled R6G-amine (blue trace) to Ag nanoparticles, showing that the signal from directly tethered R6G-amine was more intense than from physisorbed R6G<sup>+</sup>. (c) SERS detection of the neutral radical R6G-amine (R6G-amine\*) species (blue trace) made possible by EDC coupling of R6G-amine to the substrate. Reprinted with permission from ref. 32b. Copyright 2016 American Chemical Society.

together two molecules, one containing a carboxylic acid, and one containing a primary amine, by the resulting amide bond (see Fig. 7a) (ref. 32b and references therein).

Our group recently used EDC coupling to tether a rhodamine 6G (R6G) analogue containing a primary amine, *N*-(2-aminoethyl)-rhodamine 6G amide bis(trifluoroacetate) (R6G-amine), to Ag nanoparticles (NPs) to study electron transfer by electrochemical SERS (EC-SERS) (Fig. 7a). R6G cation (R6G<sup>+</sup>) adsorbs to citrate-capped Ag NPs through electrostatic interactions, but during electrochemical reduction R6G species tend to desorb. In order to detect R6G neutral radical species, we tethered R6G-amine to Ag NPs by EDC coupling with 3-mercaptopropionic acid (MPA) and 6-mercaptohexanoic acid (MHA). We compared two methods: a “heterogeneous” method, in which the Ag NPs are first fixed to a conductive substrate, functionalized with MPA or MHA and EDC-coupling with R6G-amine in the final step; and a “homogeneous” method in which the Ag NPs are functionalized with MPA or MHA and EDC-coupled with R6G-amine as a colloidal suspension, and later deposited onto a conductive substrate for EC-SERS. The homogeneous method resulted in increased numbers of SERS-active aggregates (maximized loading of

R6G-amine into hot-spots), reduced fluorescent background and increased SERS signal intensities (Fig. 7b). As expected, the MPA linker resulted in higher R6G-amine signal intensities than MHA, in agreement with the distance dependence of SERS (not shown here). Tethering R6G-amine to the surface of Ag NPs enabled the direct detection of the neutral radical species of R6G-amine (Fig. 7c).<sup>32b</sup>

A shortcoming of EDC coupling is that it requires a primary amine or carboxylic acid in the molecule of interest. Thus, EDC coupling is not a universal means of tethering molecules to SERS substrates. Additionally, for some SERS sensing applications, such as biosensing in complex biological fluids (where multiple molecules with primary amine and carboxylic acid groups are present), pre-processing of the sample to purify and extract the molecule of interest would be time-consuming and would hinder real-life application.

## 4.2 Applications of thiolated SAMs for direct and indirect SERS detection

A more generalizable and flexible approach to capturing molecules for SERS detection is to alter the surface chemistry of the SERS substrate. By functionalizing the surface with a partition layer, a molecule with low metal affinity may be brought close to the surface-enhancing substrate by attractive interactions with the partition layer. To this aim, multiple research groups have employed SAM techniques. The main advantage of a SAM is that the surface chemistry can be tailored by changing the functionality, length, and density of the monolayer. SAMs can also be short in length (<2 nm for alkanethiols containing fewer than 10 carbon atoms and <1 nm for those with fewer than 6 carbon atoms) such that direct detection of the analyte molecules attracted to the SAM is possible (the analyte is either attracted to terminal functional groups or intercalates into the SAM). SAMs can, by careful design, exploit electrostatic,<sup>33a</sup> hydrophobic,<sup>33b,c</sup> and hydrogen bonding interactions.<sup>33d,e</sup> Furthermore, mixed SAMs can take advantage of multiple types of interactions and build complexity into the surface chemistry.<sup>33d,e</sup> Beyond just attracting the molecule of interest, these multipurpose partition layers can be used to link together two different SERS substrates to increase the surface enhancement<sup>33b</sup> or to repel non-target molecules.<sup>33a</sup>

SAMs of alkanethiols are suitable for constructing a hydrophobic partition layer to attract hydrophobic molecules. Environmentally relevant polycyclic aromatic hydrocarbons (PAHs), such as pyrene, are highly hydrophobic molecules that lack any functional groups that exhibit affinity for metals. Gu *et al.* showed that by functionalizing cavities within a Ag substrate with 1,10-decanedithiol, they could create a hydrophobic surface into which PAHs readily absorb and concentrate. Following PAH absorption, this dithiol was also able to bind added Ag NPs to create plasmonic gap junctions that resulted in a high enhancement factor of 10<sup>8</sup> (resulting in a LOD of 8 nM for anthracene and 40 nM for pyrene) (Fig. 8A).<sup>33b</sup> Gu *et al.* expanded on that work to show that a SAM of an even shorter alkanethiol, hexanethiol (C6), still allowed for the absorption of PAHs. This sensing system consists of C6 on a Au film and adsorbed Au



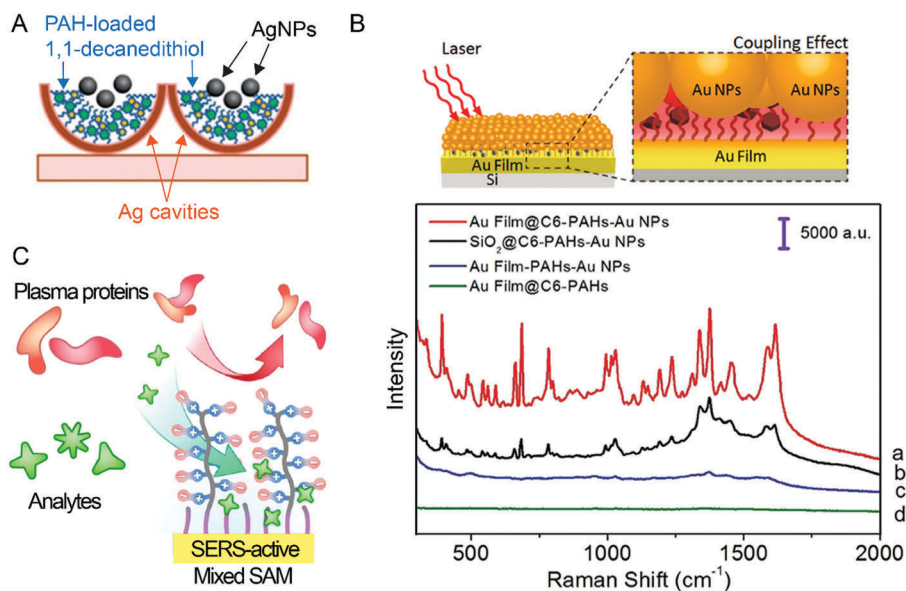


**Fig. 8** SAM SERS detection schemes. (A) Schematic illustrating the Ag cavities (red half-circles) functionalized with 1,10-decanedithiol for dual functionality: acting as a partition layer for PAHs and to link Ag NPs (gray spheres) on top of the PAH-loaded partition layer. (B) Top: Schematic illustrating the “gap-mode” SERS construct of a Au film with PAHs adsorbed into a hexanethiol (C6) partition layer, topped with adsorbed Au nanoparticles (NPs). Bottom: SERS spectra showing that PAHs are not detectable in the absence of a plasmonically-enhancing nanomaterial (Au NPs) (d, green trace), nor are PAHs detectable with Au NPs in the absence of a partition layer (c, blue trace). Both the C6 partition layer and the Au NPs are necessary to detect PAHs (b, black trace), and the highest signal is obtained when C6-PAHs-Au NPs are combined with the Au film to create plasmonic gap junctions, (a, red trace). (C) Schematic illustrating the hierarchical mixed SAM consisting of analyte-attracting functional thiols (or probing molecules) and a zwitterionic polymer brush (PCBAA modification) to both repel proteins away the SERS substrate and attract analytes. Reprinted and adapted with permission from (A) (ref. 33b) (B) (ref. 33c) (C) (ref. 33a). Copyright Royal Society of Chemistry 2013, 2016 American Chemical Society. Macmillan Publishers Ltd: *Nat. Commun.* ref. 33a, copyright 2016.

nanoparticles on top of the PAH-loaded C6 partition layer (Fig. 8B).<sup>33c</sup> The SERS spectra shown in Fig. 8B illustrate the role of each component of this sensing system: the green trace (Au film@C6-PAHs) shows that the Au film by itself is non-enhancing, necessitating the introduction of the Au NPs. The blue trace (Au film-PAHs-Au NPs) demonstrates the necessity of the partition layer – without it, PAHs are not detectable. The black (SiO<sub>2</sub>@C6-PAHs-Au NPs) and red (Au film@C6-PAHs-Au NPs) traces both demonstrate that with the partition layer and the surface-enhancing Au NPs, PAHs become detectable – but that the signal-to-noise ratio is highest when “gap mode” SERS is employed (Au film@C6-PAHs-Au NPs), as a result of the higher EF imparted by the hot-spots formed between the Au NPs and Au film.

For more selective analyte capture, a SAM of mixed monomer function can be employed. Glucose and similar monosaccharides do not bind to metals, but the detection of glucose is critical to monitoring blood sugar to treat diabetes. Our group demonstrated that a mixed SAM of different length and function, 6-mercapto-1-hexanol (MH) and decanethiol (DT), created a partition layer in which there were depth pockets containing the alcohol functional group into which glucose was able to intercalate.<sup>33d</sup> This mixed SAM allowed direct detection of glucose due to the short length of the monomer units (<2 nm). Moreover, it was suitable and stable (for two weeks) for *in vivo* glucose SERS sensing by subcutaneously implanting a SAM functionalized Ag FON into rats.<sup>33e</sup> The observed long-term

stability of the thiolated SAM in a biological system was a promising indicator of the suitability of such SAMs for bio-sensing applications.

Besides aliphatic thiols and alcohols, assemblies can also be prepared with monomers containing polarizable functional groups, such as aromatic rings, and multiple terminal functional groups. This versatility was exploited by Sun and Hung *et al.*, as well as by our own group. We showed that glucose can be indirectly detected by SERS within physiological concentration ranges and pH using a multiple terminal functional groups SAM of bis-4-amino-3-fluorophenylboronic acid,<sup>33f</sup> and Sun and Hung *et al.* showed that hierarchical mixed SAMs composed of analyte-attracting and anti-biofouling monomers (schematic shown in Fig. 8C) are adequate, robust and customizable for *in vivo* SERS sensing. In particular, for continuous drug monitoring in blood plasma, Sun and Hung *et al.* used as analyte-attracting monomers mixtures of mercaptopropionic acid and propanethiol, to enrich the analyte out of complex matrix, with an initiator from which a brush-like zwitterionic anti-biofouling layer (poly(carboxybetaine)) was grown. This anti-biofouling layer repelled components of blood plasma and prevented protein buildup around the implanted Au substrate, which would otherwise render the SERS sensor inactive. Alternatively, with different capture agents in the hierarchical mixed SAMs, Sun and Hung *et al.* demonstrated that detecting pH changes (with 4-mercaptobenzoic acid as the capture agent) and fructose (with 4-mercaptophenylboronic acid as the capture agent) is possible in undiluted human plasma.

In this case, fructose and pH sensing detection was performed indirectly, based on changes in the capture agent spectral features after protonation or interaction with fructose.<sup>33a</sup>

Unfortunately, SERS indirect sensing enabled by SAMs suffers from limited selectivity. Commonly, perturbations to the partition layer spectral features are not pronounced enough to distinguish between multiple analytes and requires careful spectral processing and chemometrics analysis, such as PCA and HCA. Yet, SAMs enable the detection of analytes with small Raman cross-sections and clearly have a crucial role in biosensing.

### 4.3 Cage-shaped molecular recognition hosts for analyte capture

One way to increase the number of affinity interactions between the capture agent and analyte molecule while maintaining short distance from the surface is to use short cage-shaped molecular recognition agents such as a cucurbit[*n*]uril (CB[*n*]), calix[*n*]arenes, or cyclodextrin (CD). These molecules have an approximately cylindrical morphology, heights of <3 nm, and serve as high-affinity hosts for a wide variety of guest molecules due to a mixture of hydrophobic and electrostatic interactions. Here we highlight examples in which SERS detection of non-metal-affinitive molecules were enabled by CB[*n*] (small organic and organometallic<sup>34b</sup>) calix[*n*]arenes (PAHs<sup>34c</sup>), and CD (antibiotics<sup>34g</sup>). Our focus on cage-like host molecules stems from their small size and potential for multiple interactions with guest molecules. A potential limitation to these capture agents is that they are relatively good Raman scatterers, and consequently, spectral features inherent to the capture agent can mask those of the analyte.

CB[*n*] molecules readily adsorb to Au surfaces through the net interaction of multiple carbonyls at each end of the molecule and form stable monolayers. Like dithiols, the symmetry of CB[*n*] molecules can be used to create hot-spots between plasmonic materials by the interactions of each end of a CB[*n*] molecule to a metal nanostructure (Fig. 9a). The guest molecule can be “loaded” into the CB[*n*] either before the introduction of the SERS substrate (“pre-mixing”), or after the CB[*n*] has adsorbed to the substrate (leaving the non-binding end open). Of the many molecules that CB[*n*] variants are able to host, only a few have been detected by SERS to date. CB[7] and CB[8] in particular have been used in SERS applications, resulting in direct detection of methyl viologen, and indirect detection of other small aromatic organic compounds (Fig. 9).<sup>34a,b</sup> The peaks in Fig. 9b labeled with asterisks are those attributable to the guest molecules. The CB[*n*] cavity deforms when it accommodates a guest molecule; this deformation is detectable by the shifting of CB[*n*] vibrational modes, particularly the 830 cm<sup>-1</sup> and 440 cm<sup>-1</sup> ring scissor and breathing modes, respectively. Fig. 10 illustrates the unique shifting of the 440 cm<sup>-1</sup> vibrational mode of CB[7] with different guests. The strength of the interaction between CB[7] and the guest molecule can also be inferred from this shifting by comparing the area of the shifted 440 cm<sup>-1</sup> peak to that of the unfilled CB[7] (Fig. 10c) (ref. 34b and references

therein). Thus, depending on the guest molecule, CB[*n*] capture agents can be used for direct or indirect sensing.

An advantage of calix[*n*]arenes over CB[*n*]s is that they can be easily thiolated, enabling a stable tethering of the host molecule to the SERS substrate. The highly hydrophobic cavity of a calix[*n*]arene makes it an inviting environment for hydrophobic molecules, similar to that of alkanethiol SAMs. Therefore, calix[*n*]arenes have also been used to detect PAHs with LODs as low as 300 pM on Ag colloids embedded in a silane xerogel matrix<sup>34c</sup> and 500 pM on a Au NP film.<sup>34d</sup>

Like calix[*n*]arenes, cyclodextrins (CDs) can be synthetically thiolated,<sup>34e</sup> or some of the alcohol groups can be oxidized to carbonyls<sup>34g</sup> to facilitate adsorption to metal surfaces. Due to the alcohol groups on each sugar monomer, the cavities formed by a CD are hydrophilic and have been used to detect

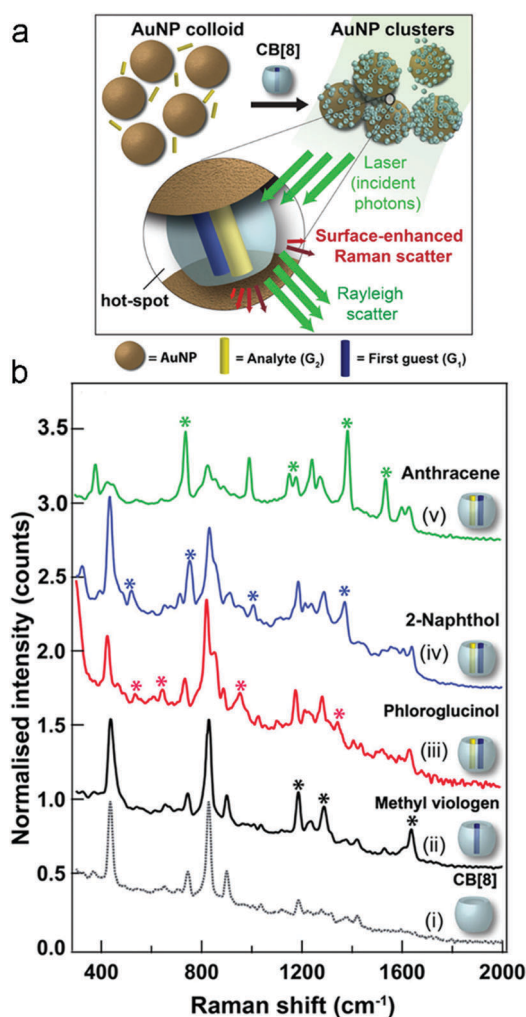


Fig. 9 Direct SERS detection of analytes enabled by cucurbit[8]uril. (a) Illustration of plasmonic nanoparticle junction formed by guest-complexed CB[8] adsorbing to two Au nanoparticles (Au NP). (b) SERS of CB[8] and various analytes captured in the CB[8] cavity. Peaks labeled with asterisks (\*) are attributable to vibrational modes of the analyte molecules, indicating direct detection of the analytes by their capture in the CB[8] cavity. Reprinted and adapted with permission from ref. 34a. Copyright 20126 American Chemical Society.

insecticides,<sup>34e</sup> polychlorinated biphenyls,<sup>34f</sup> and sulfonamide antibiotics.<sup>34g</sup>

**CAESERS concluding remarks.** In this section, we highlighted three types of short-distance capture strategies to detect by SERS molecules that do not exhibit affinity for metal nanostructures. In the first strategy, direct tethering, the analyte is chemically modified to achieve minimal length distance for direct sensing. The main limitation to this strategy is the requirement of certain functional groups in the molecule of interest. The second, was the use of thiolated SAMs to change the surface chemistry of the plasmonic metal nanostructure, creating a new environment to which molecules of interest are attracted. The strength of this strategy is the versatility of the SAMs for creating different chemical and anti-biofouling environments. The third strategy was the use of cage-like molecular recognition “host” molecules that bind to plasmonic metal nanostructures and provide a cavity that analyte molecules can fill. These capture agents exhibit similar strengths to SAMs, and are an emerging class of capture agent to be harnessed.

## 5. Future directions

We expect that advances in synthetic chemistry and materials engineering will continue to provide new directions for answering chemical questions by SERS with increased sensitivity and selectivity. We illustrate in Fig. 11 research that we anticipate will combine the advancements in UV-SERRS, plasmonic substrates, and analyte capture strategies to overcome weak Raman scattering cross-sections and reach low limits of detection for small molecules and biomolecules. In our vision, such synergistic combinations will enable the study of industrial catalysts or biologically relevant systems in extreme (*operando* SERS) or native (CAESERS in biofluids) conditions, respectively.

*Operando* SERS and CAESERS have progressed as research fields without much co-development. This disconnect is surprising, as both fields require greater sensitivity so that lower LODs can be reached to detect molecules with small Raman cross-sections. For *operando* SERS, characterizing reductive chemistry of well-known systems like ethylene on Pt(111) can be ideal to move towards studying more complicated plasmonically-enhanced or redox-enabled chemistry and chemically complex catalysts relevant to industry. In the case of bioanalytical applications of SERS, there is a great need for better ways to monitor, quantify, and interrogate biomarkers in native samples at physiological levels (ranging from nM to low mM depending on the analyte), which commonly necessitates the use of capture agents. One possible route to converging the development of *operando* SERS with CAESERS could be by exploiting resonance enhancement effects (SERRS). As resonance Raman scattering cross-sections can be five to six orders of magnitude higher than non-resonant cross-sections, this is potentially a highly beneficial research direction. Using aluminum plasmonics, the EM enhancement near the resonance conditions of many small catalytically relevant molecules (*e.g.*, ethylene) and biomolecules (*e.g.*, ubiquitin) is attainable. Despite the challenge to circumvent photodamage by UV radiation, we believe that UV-SERRS is worth exploring and that there is room for substrates optimization.

To make *operando* SERS an industrially viable technique, certain requirements must be met. Specifically: (1) robustness of the entire chemical system of interest (including plasmonic substrate, capture or spacer layer and catalysts), (2) reproducibility of the entire sensing platform fabrication, and (3) sensitivity to the catalytic reaction species of interest. Solving these issues using scalable and industry-compatible techniques outside of academic research labs remains a challenge. Many methods for stabilizing plasmonic substrates have been reported, including polymers, oxides (not limited to silica, alumina and titania) and other types

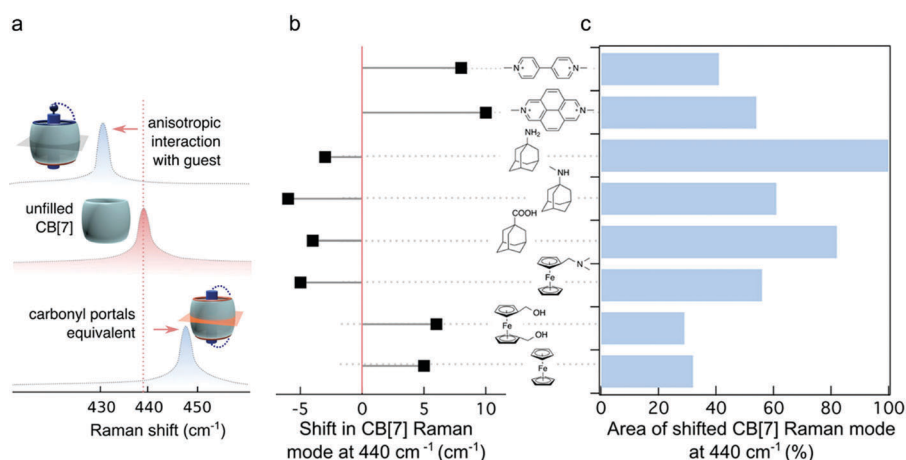


**Fig. 10** Indirect SERS detection of analytes enabled by cucurbit[7]uril. (a) Illustration of CB[7] 440 cm<sup>-1</sup> vibrational mode perturbation with guest complexation and a proposed explanation for why some analytes blue vs. red shift the 440 cm<sup>-1</sup> vibrational mode of CB[7]. (b) The unique magnitude of the 440 cm<sup>-1</sup> mode shifting for different analytes leads to the ability to distinguish between them. (c) The area of the shifted 440 cm<sup>-1</sup> mode compared to that of unfilled CB[7]; this provides some insight into the affinity between CB[7] and the analyte molecule. Reprinted and adapted with permission from ref. 34b. Copyright 2016 American Chemical Society.



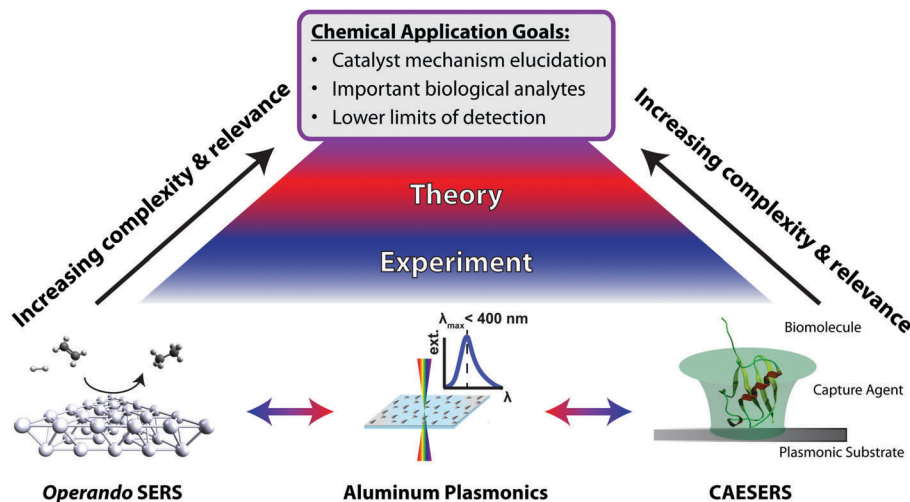


**Fig. 11** Future chemical applications of SERS driven by new synthetic chemistry and nanomaterials engineering. The topics discussed in this review are allowing new directions for exploring important catalytic and biological systems at operational catalytic and physiological biological concentrations. The road to the chemical application goals requires both experiment and theory to understand complex relevant systems.

of coatings,<sup>4</sup> but no clear consensus has been determined regarding the extent to which they actually prevent metal surface reconstruction. Surface reconstruction is exacerbated at hot-spots and goes hand-in-hand with SERS reproducibility. While the fabrication of SERS substrates with reproducible average EFs under ambient conditions is currently feasible,<sup>20</sup> most catalytic reactions take place in extreme conditions (high temperature and pressure). This suggests that nanomaterials engineering efforts beyond plasmonic properties and selectivity through capture layers also need to account for robustness (mechanical and chemical) of the entire sensing system.

Most reports that acknowledge hot-spot degradation are focused on Au or Ag, and to the best of our knowledge the stability of Al is not yet fully known (ref. 4 and 38 and references therein). Nevertheless, when aluminum is used as the plasmonic substrate, the native alumina oxide layer could serve a dual purpose as a spacer layer (due to its high uniformity) to separate the catalytic reaction from the plasmonic surface, and as a protective layer to provide stability.<sup>28,30</sup>

For sensing platforms in which the aforementioned obstacles are resolved, an unfortunate reality of *operando* SERS is the complexity of the chemical system. A common structural motif includes: (1) a plasmonic substrate which is, from a crystallographic perspective, highly heterogeneous, (2) a spacer layer to prevent the plasmonic substrate from interacting with the catalytic chemistry of interest, (3) a catalyst deposited on the spacer layer, (4) the reactants, products, and solvent or carrier gas of the catalytic chemistry. This complexity poses a challenge for accurately modeling the system. Because of the size and complexity of the system, coarse grain methods to reduce dimensionality come to mind, but accurately parameterizing the interactions of a reactive system can be highly difficult.

CAESERS by itself still faces many of the aforementioned challenges. In particular, it is important to design CAESERS sensing systems in which the capture agent is situated in a

reproducible location, preferably within a hot-spot, in order to reliably reach lower limits of detection.<sup>39</sup> The design of capture agents that minimize distance between hot-spot and analyte, exhibit strong affinity for the analyte, and are selective for specific analytes, will push this field forward and enable new sensing applications of SERS to a variety of non-metal-binding analytes. Furthermore, coupling strong electromagnetic enhancement with RRS in the UV, where many biological analytes have some absorbance, may further bolster efforts at detecting biologically relevant molecules by SERS.

## 6. Conclusions

Advances in synthetic chemistry and materials engineering have helped expand the applications of SERS beyond those in which the molecules bind to metal nanostructures and are resonant in the visible wavelength region. Capture agents bring low metal-affinity analytes close to plasmonic surfaces where large electromagnetic enhancement allows signal amplification, thereby expanding the library of molecules detectable by SERS, including molecules of biological and clinical relevance. *Operando* SERS has shown the remarkable ability to observe catalytic intermediates *via* SERS detection. However, both CAESERS and *operando* SERS have limitations for small or non-aromatic molecules due to their low non-resonant Raman scattering cross-sections. One method that may overcome this difficulty is UV-SERRS. Using aluminum plasmonics and UV excitation, where most molecules present augmented Raman cross-sections, could facilitate higher sensitivity of relevant biological and catalytic species.

The road to solving prominent catalytic and biological reaction mechanisms by SERS has only just been realized by advances in instrumentation (UV, electrochemical, super-resolution imaging, and *operando* customized Raman spectrometers) as well

as in capture layers and substrate design. Yet many questions remain: how will researchers reproducibly fabricate robust SERS substrates with UV enhancement? How can complex biological and catalytic SERS systems be modeled accurately? What is the ultimate limit of detection (LOD) for quantifying biomolecules, and how far can the LOD be pushed to measure reaction mechanisms by SERS? While there are challenges ahead, SERS researchers have clearly adopted unique and interdisciplinary strategies from fields of synthetic chemistry and materials engineering that are successfully expanding SERS in new directions. We eagerly await the next breakthroughs from these fields in the near future.

## Abbreviations

1,1-DCE	1,1-Dichloroethene
ALD	Atomic layer deposition
Al	Aluminum
Ag	Silver
Au	Gold
BBA	Bis-4-amino-3-fluorophenylboronic acid
BPE	<i>trans</i> -1,2-Bis(4-pyridyl)-ethylene
C6	Hexanethiol
CAESERS	Capture agent-enabled surface enhanced Raman spectroscopy
CB[n]	Cucurbit[n]uril
CD	Cyclodextrin
DMACl	Dimethylaluminum chloride
DT	Decanethiol
EC-SERS	Electrochemical surface-enhance Raman spectroscopy
EDC	1-Ethyl-3-(3-dimethylaminopropyl)carbodiimide
FDTD	Finite-difference time-domain
FON	Film-over-nanospheres
HCA	Hierarchical cluster analysis
LOD	Limit of detection
LSPR	Localized surface plasmon resonance
MBA	4-Mercaptobenzoic acid
MH	6-Mercapto-1-hexanol
MHA	6-Mercaptohexanoic acid
MPA	3-Mercaptopropanoic acid
MPBA	4-Mercaptophenylboronic acid
NIR	Near infrared
NP	Nanoparticle
PAHs	Polycyclic aromatic hydrocarbon
PCA	Principal components analysis
PMN	Plasmonic metal nanostructure
Ru(bpy) <sub>3</sub> <sup>2+</sup>	Tris(bipyridine)ruthenium(II)
SEM	Scanning electron microscopy
SAM	Self-assembled monolayer
SERS	Surface enhanced Raman scattering
SERRS	Surface-enhanced resonance Raman scattering
TMA	Trimethylaluminum
UV	Ultraviolet

## Acknowledgements

M. F. C., G. C. S. and R. P. V. D. acknowledge financial support from the National Science Foundation Materials Research Science and Engineering Center (DMR-1121262). R. A. H., P. C. S., G. C. S. and R. P. V. D. acknowledge financial support from Northwestern University Institute for Catalysis in Energy Processes (ICEP). ICEP is funded through the U.S. Department of Energy, Office of Basic Energy Sciences (Award Number DE-FG02-03ER15457). M. O. M. acknowledges support from the National Science Foundation Graduate Research Fellowship Program (DGE-0824162). E. V. E. acknowledges support from the National Science Foundation Graduate Research Fellowship Program (DGE-1324585). This material is based on research sponsored by the Air Force Research laboratory under agreement number FA8650-15-2-5518. The U.S. Government is authorized to reproduce and distribute reprints for Governmental purposes notwithstanding any copyright notation thereon. The views and conclusions contained herein are those of the authors and should not be interpreted as necessarily representing the official policies or endorsements, either expressed or implied, of Air Force Research Laboratory or the U.S. Government.

## References

- 1 L. R. Etchegoin, *Principles of Surface-Enhanced Raman Spectroscopy and Related Plasmonic Effects*, Elsevier Science, Amsterdam, 2008.
- 2 (a) S. A. Asher, *Ultraviolet Raman Spectroscopy*, ed. J. M. Chalmers and P. R. Griffiths, John Wiley & Sons, London, 2002; (b) S. A. Oladepo, K. Xiong, Z. Hong and S. A. Asher, Elucidating Peptide and Protein Structure and Dynamics: UV Resonance Raman Spectroscopy, *J. Phys. Chem. Lett.*, 2011, 2(4), 334–344.
- 3 A. B. Zrimsek, N. Chiang, M. Mattei, S. Zaleski, M. O. McAnally and C. T. Chapman, *et al.*, Single-Molecule Chemistry with Surface- and Tip-Enhanced Raman Spectroscopy, *Chem. Rev.*, 2016, 117(11), 7583–7613.
- 4 N. L. Gruenke, M. F. Cardinal, M. O. McAnally, R. R. Frontiera, G. C. Schatz and R. P. Van Duyne, Ultrafast and nonlinear surface-enhanced Raman spectroscopy, *Chem. Soc. Rev.*, 2016, 45(8), 2263–2290.
- 5 (a) S. S. Masango, R. A. Hackler, N. Large, A. I. Henry, M. O. McAnally and G. C. Schatz, *et al.*, High-Resolution Distance Dependence Study of Surface-Enhanced Raman Scattering Enabled by Atomic Layer Deposition, *Nano Lett.*, 2016, 16(7), 4251–4259; (b) R. A. Hackler, M. O. McAnally, G. C. Schatz, P. C. Stair and R. P. Van Duyne, Identification of Dimeric Methylalumina Surface Species during Atomic Layer Deposition Using Operando Surface-Enhanced Raman Spectroscopy, *J. Am. Chem. Soc.*, 2017, 139(6), 2456–2463.
- 6 B. Sharma, M. Fernanda Cardinal, S. L. Kleinman, N. G. Greeneltch, R. R. Frontiera and M. G. Blaber, *et al.*, High-performance SERS substrates: advances and challenges, *MRS Bull.*, 2013, 38(8), 615–624.

- 7 T. Dörfer, M. Schmitt and J. Popp, Deep-UV surface-enhanced Raman scattering, *J. Raman Spectrosc.*, 2007, **38**(11), 1379–1382.
- 8 J. Gersten and A. Nitzan, Electromagnetic theory of enhanced Raman scattering by molecules adsorbed on rough surfaces, *J. Chem. Phys.*, 1980, **73**(7), 3023–3037.
- 9 G. Kovacs, R. Loutfy, P. Vincett, C. Jennings and R. Aroca, Distance dependence of SERS enhancement factor from Langmuir-Blodgett monolayers on metal island films: evidence for the electromagnetic mechanism, *Langmuir*, 1986, **2**(6), 689–694.
- 10 Q. Ye, J. Fang and L. Sun, Surface-enhanced Raman scattering from functionalized self-assembled monolayers. 2. Distance dependence of enhanced Raman scattering from an azobenzene terminal group, *J. Phys. Chem. B*, 1997, **101**(41), 8221–8224.
- 11 G. Compagnini, C. Galati and S. Pignataro, Distance dependence of surface enhanced Raman scattering probed by alkanethiol self-assembled monolayers, *Phys. Chem. Chem. Phys.*, 1999, **1**(9), 2351–2353.
- 12 B. Kennedy, S. Spaeth, M. Dickey and K. Carron, Determination of the distance dependence and experimental effects for modified SERS substrates based on self-assembled monolayers formed using alkanethiols, *J. Phys. Chem. B*, 1999, **103**(18), 3640–3646.
- 13 J. R. Anema, J.-F. Li, Z.-L. Yang, B. Ren and Z.-Q. Tian, Shell-Isolated Nanoparticle-Enhanced Raman Spectroscopy: Expanding the Versatility of Surface-Enhanced Raman Scattering, *Annu. Rev. Anal. Chem.*, 2011, **4**(1), 129–150.
- 14 M. A. Bañares, Operando methodology: combination of *in situ* spectroscopy and simultaneous activity measurements under catalytic reaction conditions, *Catal. Today*, 2005, **100**(1–2), 71–77.
- 15 T. Wilke, X. Gao, C. G. Takoudis and M. J. Weaver, Surface-enhanced Raman spectroscopy as a probe of adsorption at transition metal-high-pressure gas interfaces. NO, CO, and oxygen on platinum-, rhodium-, and ruthenium-coated gold, *Langmuir*, 1991, **7**(4), 714–721.
- 16 Y. Zhang and M. J. Weaver, Application of surface-enhanced Raman spectroscopy to organic electrocatalytic systems: decomposition and electrooxidation of methanol and formic acid on gold and platinum-film electrodes, *Langmuir*, 1993, **9**(5), 1397–1403.
- 17 K. N. Heck, B. G. Janesko, G. E. Scuseria, N. J. Halas and M. S. Wong, Observing Metal-Catalyzed Chemical Reactions *in situ* Using Surface-Enhanced Raman Spectroscopy on Pd–Au Nanoshells, *J. Am. Chem. Soc.*, 2008, **130**(49), 16592–16600.
- 18 H. Kim, K. M. Kosuda, R. P. Van Duyne and P. C. Stair, Resonance Raman and surface- and tip-enhanced Raman spectroscopy methods to study solid catalysts and heterogeneous catalytic reactions, *Chem. Soc. Rev.*, 2010, **39**(12), 4820–4844.
- 19 A. V. Whitney, J. W. Elam, P. C. Stair and R. P. Van Duyne, Toward a Thermally Robust Operando Surface-Enhanced Raman Spectroscopy Substrate, *J. Phys. Chem. C*, 2007, **111**(45), 16827–16832.
- 20 N. G. Greeneltch, M. G. Blaber, A. I. Henry, G. C. Schatz and R. P. Van Duyne, Immobilized nanorod assemblies: fabrication and understanding of large area surface-enhanced Raman spectroscopy substrates, *Anal. Chem.*, 2013, **85**(4), 2297–2303.
- 21 J. D. Weatherston, N. C. Worstell and H. J. Wu, Quantitative surface-enhanced Raman spectroscopy for kinetic analysis of aldol condensation using Ag–Au core-shell nanocubes, *Analyst*, 2016, **141**(21), 6051–6060.
- 22 (a) P. Christopher and M. Moskovits, Hot Charge Carrier Transmission from Plasmonic Nanostructures, *Annu. Rev. Phys. Chem.*, 2017, **68**(1), 379–398; (b) W. Xie and S. Schlücker, Hot electron-induced reduction of small molecules on photorecycling metal surfaces, *Nat. Commun.*, 2015, **6**, 7570.
- 23 B. Sharma, M. F. Cardinal, M. B. Ross, A. B. Zrimsek, S. V. Bykov and D. Punihaole, *et al.*, Aluminum Film-Over-Nanosphere Substrates for Deep-UV Surface-Enhanced Resonance Raman Spectroscopy, *Nano Lett.*, 2016, **16**(12), 7968–7973.
- 24 (a) R. L. McCreery, in *Raman Spectroscopy for Chemical Analysis*. ed. J. D. Winefordner, John Wiley & Sons, Inc., NY, USA, 2000; (b) E. Kammer, T. Dorfer, A. Csaki, W. Schumacher, P. A. Da Costa Filho and N. Tarcea, *et al.*, Evaluation of Colloids and Activation Agents for Determination of Melamine Using UV-SERS, *J. Phys. Chem. C*, 2012, **116**(10), 6083–6091.
- 25 D. O. Sigle, E. Perkins, J. J. Baumberg and S. Mahajan, Reproducible Deep-UV SERRS on Aluminum Nanovoids, *J. Phys. Chem. Lett.*, 2013, **4**(9), 1449–1452.
- 26 (a) B. Ren, X.-F. Lin, Z.-L. Yang, G.-K. Liu, R. F. Aroca and B.-W. Mao, *et al.*, Surface-Enhanced Raman Scattering in the Ultraviolet Spectral Region: UV-SERS on Rhodium and Ruthenium Electrodes, *J. Am. Chem. Soc.*, 2003, **125**(32), 9598–9599; (b) L. Cui, A. Wang, D.-Y. Wu, B. Ren and Z.-Q. Tian, Shaping and Shelling Pt and Pd Nanoparticles for Ultraviolet Laser Excited Surface-Enhanced Raman Scattering, *J. Phys. Chem. C*, 2008, **112**(45), 17618–17624; (c) Y. Yang, J. M. Callahan, T.-H. Kim, A. S. Brown and H. O. Everitt, Ultraviolet Nanoplasmonics: A Demonstration of Surface-Enhanced Raman Spectroscopy, Fluorescence, and Photodegradation Using Gallium Nanoparticles, *Nano Lett.*, 2013, **13**(6), 2837–2841.
- 27 (a) B. R. Michael and C. S. George, Radiative effects in plasmonic aluminum and silver nanospheres and nanorods, *J. Phys. D: Appl. Phys.*, 2015, **48**(18), 184004; (b) A. Yang, A. J. Hryn, M. R. Bourgeois, W.-K. Lee, J. Hu and G. C. Schatz, *et al.*, Programmable and reversible plasmon mode engineering, *Proc. Natl. Acad. Sci. U. S. A.*, 2016, **113**(50), 14201–14206.
- 28 S. K. Jha, Z. Ahmed, M. Agio, Y. Ekinici and J. F. Löffler, Deep-UV surface-enhanced resonance Raman scattering of adenine on aluminum nanoparticle arrays, *J. Am. Chem. Soc.*, 2012, **134**(4), 1966–1969.
- 29 T. Ding, D. O. Sigle, L. O. Herrmann, D. Wolverson and J. J. Baumberg, Nanoimprint lithography of Al nanovoids for



- deep-UV SERS, *ACS Appl. Mater. Interfaces*, 2014, **6**(20), 17358–17363.
- 30 X.-M. Li, M.-H. Bi, L. Cui, Y.-Z. Zhou, X.-W. Du and S.-Z. Qiao, *et al.*, 3D Aluminum Hybrid Plasmonic Nanostructures with Large Areas of Dense Hot Spots and Long-Term Stability, *Adv. Funct. Mater.*, 2017, **27**(10), 1605703.
  - 31 R. A. Alvarez-Puebla and L. M. Liz-Marzan, Traps and cages for universal SERS detection, *Chem. Soc. Rev.*, 2012, **41**(1), 43–51.
  - 32 (a) A. Grondin, D. C. Robson, W. E. Smith and D. Graham, Benzotriazole maleimide as a bifunctional reactant for SERS, *J. Chem. Soc., Perkin Trans. 2*, 2001, (11), 2136–2141; (b) S. Zaleski, M. F. Cardinal, D. V. Chulhai, A. J. Wilson, K. A. Willets and L. Jensen, *et al.*, Toward Monitoring Electrochemical Reactions with Dual-Wavelength SERS: Characterization of Rhodamine 6G (R6G) Neutral Radical Species and Covalent Tethering of R6G to Silver Nanoparticles, *J. Phys. Chem. C*, 2016, **120**(43), 24982–24991.
  - 33 (a) F. Sun, H. C. Hung, A. Sinclair, P. Zhang, T. Bai and D. D. Galvan, *et al.*, Hierarchical zwitterionic modification of a SERS substrate enables real-time drug monitoring in blood plasma, *Nat. Commun.*, 2016, **7**, 13437; (b) X. Gu, S. Tian, Q. Zhou, J. Adkins, Z. Gu and X. Li, *et al.*, SERS detection of polycyclic aromatic hydrocarbons on a bowl-shaped silver cavity substrate, *RSC Adv.*, 2013, **3**(48), 25989; (c) H. X. Gu, K. Hu, D. W. Li and Y. T. Long, SERS detection of polycyclic aromatic hydrocarbons using a bare gold nanoparticles coupled film system, *Analyst*, 2016, **141**(14), 4359–13465; (d) D. A. Stuart, J. M. Yuen, N. Shah, O. Lyandres, C. R. Yonzon and M. R. Glucksberg, *et al.*, In Vivo Glucose Measurement by Surface-Enhanced Raman Spectroscopy, *Anal. Chem.*, 2006, **78**(20), 7211–7215; (e) K. Ma, J. M. Yuen, N. C. Shah, J. T. Walsh Jr., M. R. Glucksberg and R. P. Van Duyne, In vivo, transcutaneous glucose sensing using surface-enhanced spatially offset Raman spectroscopy: multiple rats, improved hypoglycemic accuracy, low incident power, and continuous monitoring for greater than 17 days, *Anal. Chem.*, 2011, **83**(23), 9146–9152; (f) B. Sharma, P. Bugga, L. R. Madison, A. I. Henry, M. G. Blaber and N. G. Greenelch, *et al.*, Bisboronic Acids for Selective, Physiologically Relevant Direct Glucose Sensing with Surface-Enhanced Raman Spectroscopy, *J. Am. Chem. Soc.*, 2016, **138**(42), 13952–13959.
  - 34 (a) S. Kasera, F. Biedermann, J. J. Baumberg, O. A. Scherman and S. Mahajan, Quantitative SERS using the sequestration of small molecules inside precise plasmonic nanoconstructs, *Nano Lett.*, 2012, **12**(11), 5924–5928; (b) D. O. Sagle, S. Kasera, L. O. Herrmann, A. Palma, B. de Nijs and F. Benz, *et al.*, Observing Single Molecules Complexing with Cucurbit[7]uril through Nanogap Surface-Enhanced Raman Spectroscopy, *J. Phys. Chem. Lett.*, 2016, **7**(4), 704–710; (c) Y.-H. Kwon, K. Sowoidnich, H. Schmidt and H.-D. Kronfeldt, Application of calixarene to high active surface-enhanced Raman scattering (SERS) substrates suitable for *in situ* detection of polycyclic aromatic hydrocarbons (PAHs) in seawater, *J. Raman Spectrosc.*, 2012, **43**(8), 1003–1009; (d) X. Shi, Y.-H. Kwon, J. Ma, R. Zheng, C. Wang and H. D. Kronfeldt, Trace analysis of polycyclic aromatic hydrocarbons using calixarene layered gold colloid film as substrates for surface-enhanced Raman scattering, *J. Raman Spectrosc.*, 2013, **44**(1), 41–46; (e) J. Wang, L. Kong, Z. Guo, J. Xu and J. Liu, Synthesis of novel decorated one-dimensional gold nanoparticle and its application in ultra-sensitive detection of insecticide, *J. Mater. Chem.*, 2010, **20**(25), 5271; (f) C. Zhu, G. Meng, Q. Huang, Z. Li, Z. Huang and M. Wang, *et al.*, Large-scale well-separated Ag nanosheet-assembled micro-hemispheres modified with HS-[small beta]-CD as effective SERS substrates for trace detection of PCBs, *J. Mater. Chem.*, 2012, **22**(5), 2271–2278; (g) L. Ouyang, L. Zhu, Y. Ruan and H. Tang, Preparation of a native  $\beta$ -cyclodextrin modified plasmonic hydrogel substrate and its use as a surface-enhanced Raman scattering scaffold for antibiotics identification, *J. Mater. Chem. C*, 2015, **3**(29), 7575–7582; (h) C. Pezzato, S. Maiti, J. L. Y. Chen, A. Cazzolaro, C. Gobbo and L. J. Prins, Monolayer protected gold nanoparticles with metal-ion binding sites: functional systems for chemosensing applications, *Chem. Commun.*, 2015, **51**(49), 9922–9931; (i) D. Jimenez de Aberasturi, J.-M. Montenegro, I. Ruiz de Larramendi, T. Rojo, T. A. Klar and R. Alvarez-Puebla, *et al.*, Optical Sensing of Small Ions with Colloidal Nanoparticles, *Chem. Mater.*, 2012, **24**(5), 738–745.
  - 35 J. Yoon, N. Choi, J. Ko, K. Kim, S. Lee and J. Choo, Highly sensitive detection of thrombin using SERS-based magnetic aptasensors, *Biosens. Bioelectron.*, 2013, **47**, 62–67.
  - 36 Y. Wang, L. J. Tang and J. H. Jiang, Surface-enhanced Raman spectroscopy-based, homogeneous, multiplexed immunoassay with antibody-fragments-decorated gold nanoparticles, *Anal. Chem.*, 2013, **85**(19), 9213–9220.
  - 37 J. Ando, M. Asanuma, K. Dodo, H. Yamakoshi, S. Kawata and K. Fujita, *et al.*, Alkyne-tag SERS screening and identification of small-molecule-binding sites in protein, *J. Am. Chem. Soc.*, 2016, **138**(42), 13901–13910.
  - 38 F. Benz, M. K. Schmidt, A. Dreismann, R. Chikkaraddy, Y. Zhang and A. Demetriadou, *et al.*, Single-molecule optomechanics in “picocavities”, *Science*, 2016, **354**(6313), 726–729.
  - 39 Y. Fang, N.-H. Seong and D. D. Dlott, Measurement of the Distribution of Site Enhancements in Surface-Enhanced Raman Scattering, *Science*, 2008, **321**(5887), 388–392.